Journal of Statistical Physics, Vol. 71, Nos. 3/4, 1993

Diffusive Description of Lattice Gas Models

Thomas Fiig[1] **and Henrik Jeldtoft Jensen**[2, 3]

Received July 9, 1992; final November 19, 1992

We have investigated a lattice gas model consisting of repulsive particles following deterministic dynamics. Two versions of the model are studied. In one case we consider a finite open system in which particles can leave and enter the lattice over the edge. In the other case we use periodic boundary conditions. In both cases the density fluctuations exhibit a $1/f$ power spectrum. The individual particles behave asymptotically like ordinary random walkers. The collective behavior of these particles shows that due to the deterministic dynamics the particles behave as if they are correlated in time. We have numerically investigated the power spectrum of the density fluctuations, the lifetime distribution, and the spatial correlation function. We discuss the appropriate Langevin-like diffusion equation which can reproduce our numerical findings. Our conclusion is that the deterministic lattice gases are described by a diffusion equation without *any* bulk noise. The open lattice gas exhibits a crossover behavior as the probability for introducing particles at the edge of the system becomes small. The power spectrum changes from a $1/f$ to a $1/f^2$ spectrum. The diffusive description, proven to be valid for a moderate boundary drive, fails altogether when the drive goes to zero.

KEY WORDS: Diffusion equation; power spectra; lattice gas; exact solutions; correlation functions; lifetime distribution; single particle properties; collective properties; dynamical crossover.

1. INTRODUCTION

One of the open questions in statistical physics is how to derive effective diffusive Langevin-like equations on the basis of the microscopic interactions in a many-body system. This taks has only been achieved in very special cases, such as in simple one-dimensional models.[1]

[1] Physics Department, Risø National Laboratory, DK-4000 Roskilde, Denmark.
[2] The Niels Bohr Institute, DK-2100 Copenhagen, Denmark.
[3] Present address: Department of Mathematics, Imperial College, London SW7 2BZ, United Kingdom.

0022-4715/93/0500-0653$07.00/0

The coarse-grained hydrodynamic equations, in which all fluctuations are integrated out, can be established by considering the symmetries and conservations of the system, and assuming the existence of an appropriate regularity of the problem so that gradient expansions are possible.[2] This leads to partial differential equations such as the ordinary diffusion equation, say, of the form

$$\partial_t n = \gamma \nabla^2 n + F[n, \nabla n] \tag{1}$$

where $F[n, \nabla n]$ denotes some general function which takes care of all the higher-order terms in the expansion in n and ∇n. The fundamental problem arises when one wants to account for fluctuations. This is most often done by adding some kind of noise, consistent with the symmetries and conservations of the system, to the right-hand side of the diffusion equation

$$\partial_t n = \gamma \nabla^2 n + F[n, \nabla n] + \rho \tag{2}$$

Lacking anything better, one normally assumes the fluctuating source ρ to be a delta-correlated (in time as well as in space) Gaussian process.[3,4] Though power law distributed noise has recently been considered,[5] the important point is that the assumed form of the noise term determines the fluctuations of the system described by (2). This makes it particularly unsatisfactory that we do not know how to determine the form of the fluctuating source term from the microscopics of the considered many-body system.

Our aim in the present paper is to put this problem into perspective by presenting results for a very simple lattice gas model.[6] Consider a lattice gas consisting of hard-core nearest-neighbor repulsive particles. Particles are allowed to enter or leave the system at the edge. The behavior of the individual particles can, for instance, be characterized by the distribution of the time $D(t)$ they spend on the lattice from the time they enter from an edge until they leave. In addition, one can determine the dispersion of the particle position with time: $R^2(t) = \langle [\mathbf{r}(t) - \mathbf{r}(t=0)]^2 \rangle$. The collective behavior of the particle system is *partly* characterized by the fluctuations in the total number of particles on the system $N(t)$. The striking point is that the long-time behavior of this model [which is captured in $N(t)$] depends on the kind of microdynamics the particles follow in each time step. Studies of two-dimensional lattice gases show that the low-frequency behavior of the power spectrum $S(f)$ of $N(t)$ depends on whether the updating algorithm is stochastic or deterministic. In both cases the power spectrum displays power-law behavior

$$S(f) \propto 1/f^{\beta} \tag{3}$$

For moderate boundary drive, the deterministic lattice gas model has $\beta = 1$ (see ref. 6 and below). A similar lattice gas with hard-core repulsion drive by stochastic Monte Carlo dynamics was studied by Andersen *et al.*,[7] who found $\beta = 3/2$ in one, two, and three dimensions.

The behavior of the single-particle characteristics $D(t)$ and $R^2(t)$, however, is not sensitive to the difference between stochastic and deterministic updating. In both cases one finds scaling behavior

$$D(t) \propto 1/t^{\alpha}, \qquad R^2(t) \propto t \tag{4}$$

with $\alpha = 3/2$, which suggests that the individual particles asymptotically experience ordinary random walks.[7,4] Moreover, as the drive at the boundary becomes small, the deterministic model exhibits a crossover to $\beta = 2$. The single-particle quantities $D(t)$ and $R^2(t)$ have the same scaling behavior independent of the strength of the boundary drive.

The exponents $\alpha = \beta = 3/2$ are characteristic of noninteracting random walkers independent of dimension[7,20] and can be reproduced by a diffusion equation like (2) with a conserving bulk noise term.[14,20] The exponents $\alpha = 3/2$ and $\beta = 1$ can be reproduced, independent of dimension, by a diffusion equation like (1) driven by a white noise boundary condition without *any* bulk noise, (see refs. 12 and 14 and below). This scaling behavior is *independent* of possible nonlinear terms in the diffusion equation.[14] We do not know of any consistent diffusive description which allows us to describe the region of low boundary drive with $\alpha = 3/2$ and $\beta = 2$.

It is worthwhile to point out that any deviation from the scaling relation $\alpha + \beta = 3$ indicates that important correlations exist between the individual particles.[9] With this in mind we note that the particles in the stochastically driven model behave as if there were no correlations between the particles. Thus, the stochastic element present in each update is able to destroy the interparticle correlations produced by the interaction. This is not the case when the model is driven deterministically. Although the particles perform erratic individual motion, as seen from the random walker form of $D(t)$ and $R^2(t)$, they continue to be correlated even after many collisions. This difference is the reason why the Langevin description in terms of (2) has to assume two different kinds of fluctuating source terms for the two types of updating algorithms. We found this result difficult to anticipate.

Below we concentrate on details of the deterministic lattice gas. In

[4] The exponent α was mistakenly determined to be equal to 2 in ref. 6. The reason for this mistake and the correct determination are described in Section 4.3 of the present paper.

Section 2 we introduce the model. Section 3 contains a detailed analytic solution of the linear diffusion equation, solved in a finite region and driven with a white noise boundary condition. We calculate the density fluctuations, the spatial correlation function, the power spectrum, and the lifetime distribution. We present our simulation results in Section 4: the measured diffusion constant for tracer diffusion as well as for collective diffusion, the power spectrum, lifetime distribution, correlation functions, and the structure factor. In order to investigate the crossover in the behavior as the drive at the edge becomes small, we devote Section 4.6 to the study of crossover behavior as a function of boundary drive. In Section 5 we describe a completely deterministic periodic model which also exhibits $1/f$ fluctuations in the particle density.

2. THE MODEL

The lattice gas model is constructed to simulate particles which follow Stokesian dynamics. That is, the equation of motion has the form $\eta \mathbf{v} = \mathbf{F}$, where η is the friction coefficient, $\mathbf{v}$ the velocity, and $\mathbf{F}$ the total force acting on the particle.

Consider now a two-dimensional square lattice of $N \times N$ sites. Each site can be empty or occupied. Particles on *nearest neighbor* sites repel each other with a central force of unit strength. The dynamics is deterministic and defined in the following way. For each particle we sum up all the forces acting upon the particle in the normal vectorial fashion. If the resulting force is nonzero, we move the particle one lattice site in the direction according to the resulting force (diagonal moves are accepted). In case of competition where two particles which are acted upon by a force of equal strength want to move into the same site, neither particle moves. This will be termed the *blocking mechanism.* Finally, if two particles want to move to the same site but are acted upon by forces of unequal strength, the particle with the largest force wins. The whole lattice is simultaneously updated. The updating rules are illustrated in Fig. 1 in the case of an 8×8 lattice.

The boundary drive acts as a particle reservoir which tends to set up an external pressure by occupying the outer boundary by fixed particles (the cross-hatched particles in Fig. 1), which tends to push particles on neighbor sites into the lattice.

In each iteration, the particles at the boundary sites (i.e., the particles which are nearest neighbor to the cross-hatched particles) are annihilated, and new particles are introduced at all the boundary sites with a probability p per site.

Figure 2 shows a series of snapshots of our lattice gas model, which

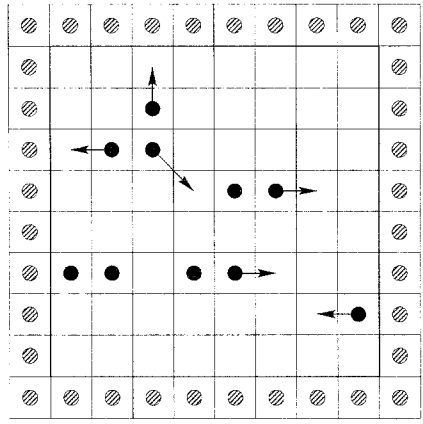

Fig. 1. Updating rules for the deterministic lattice gas model. The arrows on the particles indicate where the particles move to in the next iteration. The particles without any arrow do not move. The case where two or more particles want to enter the same site needs special consideration. First, for competition between two particles which are acted upon by a force of equal strength, no particle moves. This is shown for the four particles occupying the third row from the bottom. Second, if two particles want to move to the same site but are acted upon by forces of unequal strength, the particle with the largest force wins, as shown for the particle with the diagonal arrow.

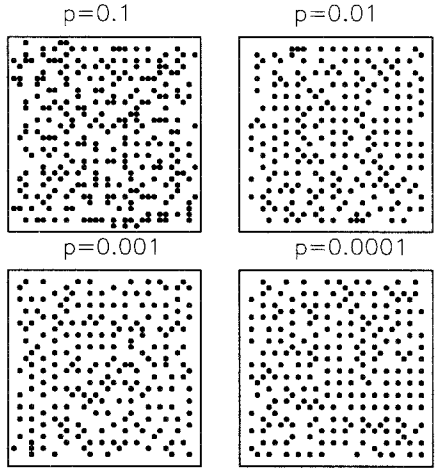

Fig. 2. Series of snapshots for a fixed lattice site of 32×32 for different values of the boundary drive p. As p is reduced, the external pressure ceases, thereby allowing the continued growth of ordered domains.

illustrates the particle configuration for a 32×32 lattice for different values of p. All snapshots are taken after the lattice gas has equilibrated. For $p = 10^{-1}$, we see the particles occupying the lattice more or less uniformly, with no observable pattern. Several of the particles are seen to be nearest neighbors, and are thus likely to move in the next iteration. Moving on to $p = 10^{-2}$, one immediately sees a difference in the configuration. Now a much smaller fraction of the particles are nearest neighbors, giving rise to the formation of domains of ordered particles sitting in a cubic lattice. It can readily be checked that the cubic pattern has a degeneracy of four. Thus, the dynamics for small p can be thought of as an interplay among domains of different types, the competition between the external drive which tends to frustrate the formation of the ordered structure and the energy-driven development of this pattern. For $p = 10^{-3}$ and finally $p = 10^{-4}$, this development continues, creating larger and larger ordered domains. In the limit of vanishing p it is expected that the lattice ends up in one monodomain extending through the lattice.

One might wonder why the nearest neighbor interaction used does not lead to a checkerboard pattern of density 1/2 at low p. The checkerboard pattern will, like the observed cubic pattern, minimize the interaction energy. However, the checkerboard pattern is unstable to perturbations. A particle displaced one site in the checkerboard pattern will produce a perturbation which propagates through the whole pattern, whereas a similar perturbation of the cubic pattern only propagates one-dimensionally.

3. DIFFUSIVE DESCRIPTION

The lattice gas described above consists of repulsive particles moving around on the lattice. We will now attempt to describe the lattice gas from a macroscopic point of view by introducing a continuous model. The application of such a model to the discrete lattice gas model is only valid at a coarse-grained level, where the microscopic motion of the particles has been averaged out. The simplest possible description one can think of is the linear diffusion equation. In order to determine to what degree the diffusion equations offers an adequate description, we introduce a coarse-grained density $n(\mathbf{r}, t)$, which denotes the number density of particles, in a volume element around $\mathbf{r}$ at time t. We will concentrate on three properties, the power spectrum $S(f)$ of the total number of particles on the lattice, the spatial correlation function $C(\mathbf{r}, \mathbf{r}')$, and the lifetime distribution $D(t)$. In order to calculate these quantities only the fluctuations in $n(\mathbf{r}, t)$ around its average value $\langle n(\mathbf{r}, t) \rangle$ enter into the calculation. Thus the absolute value of $\langle n(\mathbf{r}, t) \rangle$ is irrelevant and for convenience we will take this as zero.

The appropriate boundary condition on $n(\mathbf{r}, t)$ should be taken such as to mimic the boundary drive on the lattice gas model. In the lattice gas model, the particle density at the boundary varies in a stochastic manner, which is characterized by the lack of long-time correlations. Thus, it is natural to apply a white noise boundary condition on $n(\mathbf{r}, t)$.

The diffusion equation should be solved in a bounded region Ω, where $\Omega = [0, L] \times [0, L]$. The side length $L = Na_0$ is measured in units of the lattice spacing a_0. Hence

$$\frac{\partial n(\mathbf{r}, t)}{\partial t} = \gamma \nabla^2 n(\mathbf{r}, t) + \rho(\mathbf{r}, t) \qquad (\mathbf{r} \in \Omega,\ t > 0) \tag{5}$$

$$n(\mathbf{r}, t) = \eta(\mathbf{r}, t) \qquad (\mathbf{r} \in S,\ t > 0) \tag{6}$$

where S denotes the surface of Ω. The Dirichlet condition consists of fixing $n(\mathbf{r}, t)$ to take the value $\eta(\mathbf{r}, t)$, which is a white noise boundary term.[5]

The solution to (5) and (6) can be expressed in terms of the appropriate Green's function $G(\mathbf{r}, t \mid \mathbf{r}_0, t_0)$. The Green's function is the propagator to a pulse at $\mathbf{r}_0 \in \Omega$ at time t_0. The causality condition forces $G(\mathbf{r}, t \mid \mathbf{r}_0, t_0) = 0$ when $t < t_0$.

The Green's function is a solution to the problem involving an impulsive point source

$$\frac{\partial G(\mathbf{r}, t \mid \mathbf{r}_0, t_0)}{\partial t} - \gamma \nabla^2 G(\mathbf{r}, t \mid \mathbf{r}_0, t_0) = \delta(\mathbf{r} - \mathbf{r}_0)\, \delta(t - t_0) \qquad (\mathbf{r} \in \Omega,\ t > 0) \tag{7}$$

where the Green's function should be chosen to satisfy the homogeneous boundary condition $G(\mathbf{r}, t \mid \mathbf{r}_0, t_0) = 0$ when $\mathbf{r}_0 \in S_0$ or $\mathbf{r} \in S$.

The Green's function is now used to construct the solution for the particle density $n(\mathbf{r}, t)$ (see ref. 16, Chapter 7). Hence, in general,

$$\begin{aligned} n(\mathbf{r}, t) = & \int_0^t \int_{\Omega_0} G(\mathbf{r}, t \mid \mathbf{r}_0, t_0)\, \rho(\mathbf{r}_0, t_0)\, d\Omega_0\, dt_0 \\ & + \int_{\Omega} G(\mathbf{r}, t \mid \mathbf{r}_0, 0)\, n(\mathbf{r}_0, 0)\, d\Omega_0 \\ & + \gamma \int_0^t \int_{S_0} [G(\mathbf{r}, t \mid \mathbf{r}_0, t_0)\, \nabla_0 n(\mathbf{r}_0, t_0) \\ & - n(\mathbf{r}_0, t_0)\, \nabla_0 G(\mathbf{r}, t \mid \mathbf{r}_0, t_0)]\, dS_0\, dt_0 \end{aligned} \tag{8}$$

[5] Diffusion driven by a boundary noise was considered by Liu[10] in connection with $1/f$ noise in metals. See also the review by Duta and Horn.[11]

The first term in (8) represents the response of a volume noise term, which we will *disregard* because we are only concerned with the deterministic lattice gas model. The second term represents the effect of having an initial condition on $n(\mathbf{r}, t)$. This term can, however, be ignored, because we are only interested in ensemble properties, which we assume to be independent of the initial condition. Finally, using the homogeneous condition of the Green's function, we obtain that the first part in the third term vanishes. Hence,

$$n(\mathbf{r}, t) = -\gamma \int_0^t \int_{S_0} n(\mathbf{r}_0, t_0)\, \nabla_0 G(\mathbf{r}, t \mid \mathbf{r}_0, t_0)\, dS_0\, dt_0 \tag{9}$$

The solution to (7) may be obtained by the method of eigenfunction expansion, whereby we expand the Green's function on the eigenfunctions to the Laplacian ∇^2 on the domain Ω subject to zero homogeneous Dirichlet condition,

$$\nabla^2 u(\mathbf{r}) = \lambda u(\mathbf{r}) \tag{10}$$

The eigenfunctions and eigenvalues are obtained by the method of separation of variables.[18] Hence,

$$u_{mn} = \frac{2}{L} \sin \frac{m\pi x}{L} \sin \frac{n\pi y}{L}, \qquad \lambda_{mn} = -\left[\left(\frac{m\pi}{L}\right)^2 + \left(\frac{n\pi}{L}\right)^2\right] \tag{11}$$

where the indices m, n take the values $(m, n = 1, \ldots, \infty)$. The Green's function can now be obtained by expanding $G(\mathbf{r}, t \mid \mathbf{r}_0, t_0)$ on the eigenfunctions (11), and the Green's function can now be written

$$G(\mathbf{r}, t \mid \mathbf{r}_0, t_0) = \sum_{m=1}^{\infty} \sum_{n=1}^{\infty} u_{mn}(\mathbf{r})\, u_{mn}(\mathbf{r}_0) \exp[\gamma \lambda_{mn}(t - t_0)]\, \Theta(t - t_0) \tag{12}$$

where $\Theta(t)$ is the Heaviside step function, included to force $G = 0$ when $t < t_0$. The Green's function (12) is now to be substituted into (9) to get the formula for $n(\mathbf{r}, t)$. The noise term $\eta(\mathbf{r}, t)$ is separated into four parts, $\eta^{(i)}(\mathbf{r}, t)$, where $i = 1, \ldots, 4$ corresponds to the four boundaries of Ω.

After evaluating the gradient of the Green's function and simplifying the expression, we obtain

$$\begin{aligned} n(\mathbf{r}, t) = -\frac{2\gamma}{L} \sum_{m=1}^{\infty} \sum_{n=1}^{\infty} u_{mn}(\mathbf{r}) \int_0^t dt_0 \exp[\gamma \lambda_{mn}(t - t_0)]\, \Theta(t - t_0) \\ \times \left\{ \int_0^L dx_0 \sin\left(\frac{m\pi x_0}{L}\right)\left(\frac{n\pi}{L}\right) [\eta^{(3)}(\mathbf{r}_0, t_0) \cos(n\pi) - \eta^{(1)}(\mathbf{r}_0, t_0)] \right. \\ \left. \times \int_0^L dy_0 \sin\left(\frac{n\pi y_0}{L}\right)\left(\frac{m\pi}{L}\right) [\eta^{(2)}(\mathbf{r}_0, t_0) \cos(m\pi) - \eta^{(4)}(\mathbf{r}_0, t_0)] \right\} \end{aligned} \tag{13}$$

Now we are in a position to calculate the power spectrum and other quantities. It is important to recognize that (13) is generally valid for any boundary drive $\eta(\mathbf{r}, t)$, though here we restrict this to include only white noise. This assumption can easily be stated in terms of the correlation function between the individual noise terms. We will assume that the noise terms are uncorrelated in space and time, in correspondence with the boundary conditions for the deterministic lattice gas model, with zero average:

$$\begin{aligned} \langle \eta^{(i)}(\mathbf{r}, t)\, \eta^{(j)}(\mathbf{r}', t') \rangle &= A\delta_{ij}\delta(\mathbf{r}-\mathbf{r}')\,\delta(t-t') \\ \langle \eta^{(i)}(\mathbf{r}, t) \rangle &= 0 \end{aligned} \tag{14}$$

where $\langle \cdots \rangle$ denotes an ensemble average. The ensemble average is performed by considering a huge number of independent realizations of the white noise term $\eta^{(i)}(\mathbf{r}, t)$. The ensemble average is as usually converted to a time and space average. Thus, for any function $f(\mathbf{r}, t)$, the average $\langle f(\mathbf{r}, t) \rangle$ is calculated from

$$\langle f(\mathbf{r}, t) \rangle = \frac{1}{L^2} \int_{\Omega} d\Omega \lim_{T \to \infty} \frac{1}{T} \int_0^T dt\, f(\mathbf{r}, t) \tag{15}$$

The functional form of $\eta^{(i)}(\mathbf{r}, t)$ is not given *a priori*, but is chosen to match our needs. The actual form of $\eta^{(i)}(\mathbf{r}, t)$ we choose is

$$\begin{aligned} \eta^{(i)}(\mathbf{r}, t) &= \sum_{n=1}^{N} \eta_n^{(i)}(\mathbf{r}, t) \\ \eta_n^{(i)}(\mathbf{r}, t) &= \delta(\mathbf{r}-\mathbf{r}_n^{(i)})\, \Delta t \sum_{k=0}^{\infty} \delta(t - t_{k,n}^{(i)}) - p\delta(\mathbf{r}-\mathbf{r}_n^{(i)}) \end{aligned} \tag{16}$$

where Δt is our time unit. The expression (16) is very appealing physically, and we will explain it in the following. Consider a specific lattice site along the border i, $\mathbf{r}_n^{(i)}$, where the index n picks one of the N possible choices. The noise term acting on this site is termed $\eta_n^{(i)}(\mathbf{r}, t)$. The time sequence $\{t_{k,n}^{(i)}\}$ $(k = 0, \ldots, \infty)$ is selected in such a way that on average p elements from the series fall in each time interval of duration Δt. If we neglect the term $p\delta(\mathbf{r}-\mathbf{r}_n^{(i)})$ in $\eta_n^{(i)}(\mathbf{r}, t)$, this corresponds to a particle entering the lattice site $\mathbf{r}_n^{(i)}$ exactly when $t = t_{k,n}^{(i)}$. [The term containing p could be neglected in the whole analysis, but is included here such that the average value $\langle \eta_n^{(i)}(\mathbf{r}, t) \rangle$ is zero.] This choice is a matter of convenience, and is valid because we only consider the fluctuations in $n(\mathbf{r}, t)$. The form of the noise term $\eta^{(i)}(\mathbf{r}, t)$ is just a sum over the individual noise terms $\eta_n^{(i)}(\mathbf{r}, t)$ acting on the lattice sites.

The amplitude factor A in (14) controls the number of particles which enter the lattice over the rim and is calculated by substituting (16) into (14), using the definition of the average given by (15). By applying Campell's theorem,[19] we obtain

$$A = \frac{Np\,\Delta t}{L^2} \tag{17}$$

3.1. Power Spectrum

The power spectrum $S(f)$ of the total number of particles is evaluated from Fourier transformation of the integrated particle density given by

$$N(\omega) = \int_{-\infty}^{\infty} dt \exp(i\omega t) \int_{\Omega} d\Omega\, n(\mathbf{r}, t) \tag{18}$$

By substituting (13) into (18), we obtain

$$\begin{aligned} N(\omega) = 16\pi\gamma \sum_{m_1=1}^{\infty}{}' \sum_{n_1=1}^{\infty}{}' \frac{1}{\lambda\gamma_{m_1 n_1} + i\omega} \int_{-\infty}^{\infty} dt_0 \exp(i\omega t_0) \\ \times \left\{ \int_0^L dx_0 \sin\left(\frac{m_1 \pi x_0}{L}\right)\left(\frac{1}{m_1 L}\right) [\eta^{(1)}(\mathbf{r}_0, t_0) + \eta^{(3)}(\mathbf{r}_0, t_0)] \right. \\ \left. \times \int_0^L dy_0 \sin\left(\frac{n_1 \pi y_0}{L}\right)\left(\frac{1}{n_1 L}\right) [\eta^{(2)}(\mathbf{r}_0, t_0) + \eta^{(4)}(\mathbf{r}_0, t_0)] \right\} \end{aligned} \tag{19}$$

where the summation symbol $\sum'$ denotes that the sum indices in (19) are restricted to odd values. Further, we have changed the upper limit in the t_0 integral from t to ∞, which is allowed because of the Heaviside function in (13). The power spectrum $S(\omega)$ is obtained from

$$S(\omega)\,\delta(\omega - \omega') = \langle N(\omega)\, N^*(\omega') \rangle \tag{20}$$

The delta function in the definition (20) represents the dc component of $N(t)$. The ensemble average is handled by (14), whereby we obtain

$$\begin{aligned} \langle N(\omega)\, N^*(\omega') \rangle = \frac{512\pi^3\gamma^2 A}{La_0} \sum_{m_1=1}^{\infty}{}' \sum_{m_2=1}^{\infty}{}' \sum_{n_1=1}^{\infty}{}' \sum_{n_2=1}^{\infty}{}' \frac{\delta(\omega - \omega')}{(\lambda_{m_1 n_1}\gamma + i\omega)(\lambda_{m_2 n_2}\gamma - i\omega')} \\ \times \left[\left(\frac{1}{n_1}\right)^2 \delta_{n_1, n_2} + \left(\frac{1}{m_1}\right)^2 \delta_{m_1, m_2} \right] \end{aligned} \tag{21}$$

It should be recognized in (21) that the summation indices m_2 in the first part and n_2 in the second part collapse because of the orthogonality relation of the eigenfunctions.

The occurrence of the prefactor $1/a_0$ in (21) results because the integral over $\eta^{(i)}(\mathbf{r}_0, t_0)$ is a line integral, while the boundary noise is a particle density. This is treated by averaging $\eta^{(i)}(\mathbf{r}_0, t_0)$ over one lattice unit a_0.

The next step is to introduce the eigenvalues (11) back into (21). After some algebra we get

$$S(\omega) = \frac{512AL^3}{\pi a_0}\left[\sum_{m_1=1}^{\infty}{}' \left(\frac{1}{m_1^2}\right)\left(\sum_{n_1=1}^{\infty}{}' \frac{1}{n_1^2+m_1^2-i\omega L^2/\pi^2\gamma}\right)\right.$$
$$\times\left(\sum_{n_2=1}^{\infty}{}' \frac{1}{n_2^2+m_1^2+i\omega L^2/\pi^2\gamma}\right)+\sum_{n_1=1}^{\infty}{}' \left(\frac{1}{n_1^2}\right)\left(\sum_{m_1=1}^{\infty}{}' \frac{1}{m_1^2+n_1^2-i\omega L^2/\pi^2\gamma}\right)$$
$$\left.\times\left(\sum_{m_2=1}^{\infty}{}' \frac{1}{m_2^2+n_1^2+i\omega L^2/\pi^2\gamma}\right)\right] \tag{22}$$

The summation can now be evaluated using the identity[17]

$$\sum_{n=1}^{\infty}{}' \frac{1}{n^2-z} = \frac{\pi}{4\sqrt{z}}\tan\left(\frac{\pi\sqrt{z}}{2}\right), \qquad z\in\mathscr{C} \tag{23}$$

As can be seen from (22), the summation (23) occurs together with a summation of the complex conjugate. Putting everything together, we obtain

$$S(\omega) = \frac{64AL^3\pi}{a_0}\sum_{m=1}^{\infty}{}' \frac{1}{m^2}\frac{1}{(m^4+\omega^2L^4/\pi^4\gamma^2)^{1/2}}$$
$$\times\tan\left[\frac{\pi}{2}\left(-m^2+\frac{i\omega L^2}{\pi^2\gamma}\right)^{1/2}\right]\tan\left[\frac{\pi}{2}\left(-m^2-\frac{i\omega L^2}{\pi^2\gamma}\right)^{1/2}\right] \tag{24}$$

To continue with the calculation, we introduce the notation

$$u_m = \mathrm{Re}\left(-m^2+\frac{i\omega L^2}{\pi^2\gamma}\right)^{1/2}$$
$$v_m = \mathrm{Im}\left(-m^2+\frac{i\omega L^2}{\pi^2\gamma}\right)^{1/2} \tag{25}$$

where Re and Im are the real and the imaginary parts, respectively. It should be recognized that u_m and v_m are both positive. By introducing (25) into (24), we obtain

$$S(\omega) = \frac{64AL^3\pi}{a_0}\sum_{m=1}^{\infty}{}' \frac{1}{m^2}\frac{1}{(m^4+\omega^2L^4/\pi^4\gamma^2)^{1/2}}\frac{\cosh(\pi v_m)-\cos(\pi u_m)}{\cosh(\pi v_m)+\cos(\pi u_m)} \tag{26}$$

The minimal value of v_m occurs for $\omega = 0$, which makes $v_m = m$. Thus, $\cosh(\pi v_m) \geqslant \cosh(\pi m) \gg 1$; this means that, to a good approximation, we can disregard the term $\cos(\pi u_m)$ in both the numerator and the denominator:

$$S(\omega) \simeq \frac{64\pi AL^3}{a_0} \sum_{m=1}^{\infty}{}' \frac{1}{m^2} \frac{1}{(m^4 + \omega^2 L^4/\pi^4\gamma^2)^{1/2}} \tag{27}$$

It now turns out that only the first term $m = 1$ in (27) contributes significantly to the sum, because of the rapidly decreasing term $1/m^2$.

Substituting the formula for A in (27), we can write the final result for the power spectrum as

$$S(\omega) \simeq \frac{64\pi L^2 p\, \Delta t}{a_0^2} \frac{1}{(1 + \omega^2 L^4/\pi^4\gamma^2)^{1/2}} \tag{28}$$

which compared to (26) is accurate to within 15%. We define a characteristic frequency ω_c from (28) that will be especially important in our subsequent discussion of our computer simulations:

$$\omega_c = \gamma \left(\frac{\pi}{L}\right)^2 \tag{29}$$

From (28) it follows that for $\omega \ll \omega_c$, $S(\omega)$ is almost constant, which gives rise to white noise, while for $\omega \gg \omega_c$, we obtain $S(\omega) \propto 1/\omega$. Notice that $S(\omega = 0)$ scales with the volume of the system. This is to be expected on the following grounds. The average of the total number of particles on the lattice scales with the volume of the system; thus, $\langle N(t) \rangle \propto L^2$. Hence the fluctuation in $N(t)$ is of the order of $\Delta N(t) \sim \langle N(t) \rangle^{1/2} \propto L$. The power spectrum is expressible as the cosine transform of $\langle \Delta N(t)^2 \rangle$ (the Wiener–Khintchine theorem[21]) and is seen to scale with L^2.

It has been pointed out that $1/f$ noise would result from the driven diffusion equation[12, 14]; however, this case was for a semi-infinite system, which does not have the crossover to white noise at low frequencies. For our purpose, this finite-size effect is of particular importance because the crossover frequency is readily determined from our computer experiments, and the finite-size dependence can be checked.

3.2. Correlation Functions

We now turn to the discussion of the spatial correlation functions. The correlation between the particle numbers at position $n(\mathbf{r}, t)$ and at position

$n(\mathbf{r}', t')$ is usually described in terms of the equal-time correlation function $C(\mathbf{r}, \mathbf{r}')$ defined by

$$C(\mathbf{r}, \mathbf{r}') = \langle [n(\mathbf{r}, t) - \langle n(\mathbf{r}, t)\rangle][n(\mathbf{r}', t) - \langle n(\mathbf{r}', t)\rangle]\rangle \tag{30}$$

where $\langle \cdots \rangle$, as before, denote an ensemble average. The calculation of the correlation function is done in the same fashion as the evaluation of the power spectrum. The formula (30) can be simplified by noting that the particle density is constructed in such a way that $\langle n(\mathbf{r}, t)\rangle = 0$. Hence,

$$C(\mathbf{r}, \mathbf{r}') = \frac{2\gamma p\, \Delta t}{L^2 a_0^2} \sum_{m_1=1}^{\infty} \sum_{m_2=1}^{\infty} \sum_{n_1=1}^{\infty} \sum_{n_2=1}^{\infty} \frac{1}{m_1^2 + n_1^2 + m_2^2 + n_2^2} u_{m_1 n_1}(\mathbf{r})\, u_{m_2 n_2}(\mathbf{r}') \times \{[1 + (-1)^{n_1 + n_2}] n_1 n_2 \delta_{m_1 m_2} + [1 + (-1)^{m_1 + m_2}] m_1 m_2 \delta_{n_1 n_2}\} \tag{31}$$

In expression (31) it is necessary to introduce an ultraviolet cutoff corresponding to the smallest wavelength on our lattice, i.e., one lattice constant. This means that all sum indices takes values from 1 to N.

Figure 3 is a plot of (31) for a system size of $N = 33$. We have fixed $\mathbf{r} = (L/2, L/2)$ to the center of the lattice, while $\mathbf{r}' = (x, L/2)$ sweeps the lattice horizontally. We see oscillations with a wavelength of one lattice unit; this comes from the fact that the sum has been truncated, leaving maximum intensity on the Fourier component, corresponding to the wavelength of one lattice unit.

At a larger scale we see variation, showing that the correlation function is larger when $\mathbf{r}'$ approaches the border. To understand this behavior, notice that $\langle n(\mathbf{r}', t)\rangle = 0$, which follows from (13), while $\langle n(\mathbf{r}', t)^2\rangle$

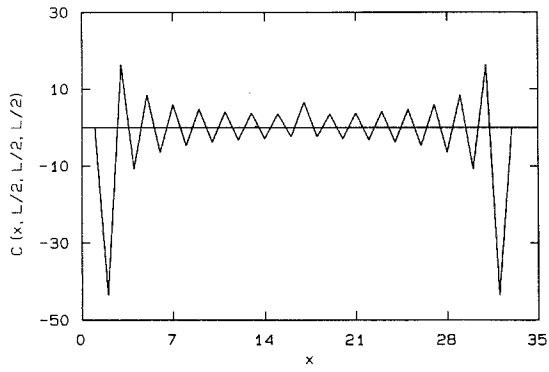

Fig. 3. Spatial correlation function $C(\mathbf{r}, \mathbf{r}')$ for $N = 33$, where $\mathbf{r}$ is fixed to the center of the lattice and $\mathbf{r}'$ sweeps the lattice horizontally.

depends on $\mathbf{r}'$, decreasing toward the center of the lattice. From this it follows that the fluctuation in the correlation function is damped toward the center of the lattice. At the center itself we see a small peak. In Section 4 we present computer simulations showing a quite different behavior.

3.3. Lifetime Distribution

The lifetime distribution characterizes the survival times of the particles on the lattice. It is defined as the ensemble average of the time each individual particle spends on the lattice. This is in general impossible to treat from a macroscopic point of view, because the path and lifetime of a particle are highly correlated with those of the other particles. In this section, we calculate the lifetime distribution from our diffusive description of the lattice gas model.

The lifetime distribution can only be calculated in a probabilistic manner, that is, we treat the particles as if they were noninteracting random walkers.

We consider a delta spike in (x_0, y_0) at time $t_0 = 0$ in the particle density and follow how the total particle probability leaks out of the domain Ω. The lifetime distribution is calculated from

$$D(t) = -\frac{\partial}{\partial t} \int_{\Omega} d\Omega\, n(\mathbf{r}, t) \tag{32}$$

The expression (32) can be simplified by introducing the diffusion equation (5) for the partial derivative. Hence,

$$D(t) = -\gamma \int_{\Omega} d\Omega\, \nabla^2 n(\mathbf{r}, t) = -\gamma \int_{S} d\mathbf{S} \cdot \nabla n(\mathbf{r}, t) \tag{33}$$

The particle density $n(\mathbf{r}, t)$ to be substituted into (33) is the Green's function given by (12), where $t_0 = 0$, whereby we obtain

$$D(t) = \frac{-16\gamma}{L^2} \sum_{m=1}^{\infty}{}' \sum_{n=1}^{\infty}{}' \sin\left(\frac{m\pi x_0}{L}\right) \sin\left(\frac{n\pi y_0}{L}\right) \times \left(\frac{n}{m} + \frac{m}{n}\right) \exp(\gamma \lambda_{mn} t)\, \Theta(t) \tag{34}$$

In our lattice gas model, particles enter over the rim, and the lifetime distribution is a simple average over all initial particle positions. To do this in Eq. (34) needs some care, because, by definition, the Green's function takes zero value on the surface $S = \partial\Omega$. This means that $D(t)$ would be

identically zero if we follow this path. To obtain a reasonable answer, we need to introduce the particle close to the surface from the bulk. The obvious choice is to choose this distance as one lattice unit a_0. The calculation, however, poses no difficulty. Hence,

$$D(t) = \frac{64\gamma a_0}{L^3} \sum_{m=1}^{\infty}{}' \sum_{n=1}^{\infty}{}' \left(\frac{n}{m} + \frac{m}{n}\right)^2 \exp(\gamma \lambda_{mn} t)\, \Theta(t) \tag{35}$$

In the following we are only concerned with the asymptotic expansion of (35). Thus it is sufficient to obtain an approximate solution.

To proceed, the double sum for the lifetime distribution can be changed to a product of single sums. Define

$$S_\alpha(a) = \sum_{n=1}^{\infty}{}' n^\alpha \exp(-an^2) \tag{36}$$

We will define a crossover time t_c, which is simply given by $t_c = 1/\omega_c$, where ω_c is the crossover frequency obtained from finite-size scaling of the power spectrum (29). Hence the lifetime distribution (35) can be written as

$$D(t) \propto S_{-2}(t/t_c)\, S_2(t/t_c) + S_0(t/t_c)^2 \tag{37}$$

The single sum (36) can be approximated by applying the Euler–Maclaurin formula.[22] Thus

$$S_\alpha(t/t_c) = \frac{1}{2} \int_1^\infty x^\alpha \exp\left(-\frac{t}{t_c} x^2\right) dx + \frac{1}{2} \exp\left(-\frac{t}{t_c}\right) + R_\alpha \tag{38}$$

We have retained the leading correction, which is just the function $x^\alpha \exp(-ax^2)$ evaluated at the boundary values of the integral, but we will disregard higher-order corrections R_α. The integrals are all expressible in terms of the error function [ref. 23, formula (3.461.5)]. Putting everything together, we find

$$D(t) \propto \exp(-2t/t_c)(t/t_c)^{-3/2} \tag{39}$$

From (39) we see that there exists a region where the lifetime distribution follows an algebraic scaling law with exponent 1.5, independent of lattice size. This is due to the fact that the error function is slowly varying compared to the algebraic term. For times t larger than some characteristic value t_c, the distribution falls off exponentially. This crossover comes from the finite size of the system and t_c is shown to scale with the volume of the lattice.

4. RESULTS OF COMPUTER SIMULATION

In this section we describe the results of computer simulations of the deterministic lattice gas model introduced in Section 2. In the mathematical formulation of the model used in the computer simulations we introduce a discrete variable $z(\mathbf{r}, t)$, which is analogous to the particle density $n(\mathbf{r}, t)$ used in the diffusive description. Let $z(\mathbf{r}, t) = 0$ if the lattice site $\mathbf{r} = (i, j)$ at time t is empty; otherwise we set $z(\mathbf{r}, t) = 1$. The individual particle path through the lattice will be denoted $\mathbf{r}(t)$. Thus the particle enters at the boundary at position $\mathbf{r}(t = 0)$. The particle then diffuses around and at a later moment t' is annihilated. The time t' is termed the *lifetime* of the particle.

4.1. Diffusion Constant

In the description of the continuous model of the lattice gas, there enter two parameters: the amplitude of the white noise A, which was discussed in Section 3, and the diffusion constant γ. The lattice gas model has, however, only one free parameter, p. Thus we expect that γ is some function of p.

We have calculated the *tracer* diffusion coefficient D by measuring the ensemble average of the mean square displacement $R^2(t)$ of the particles,

$$R^2(t) = \langle [\mathbf{r}(t) - \mathbf{r}(t = 0)]^2 \rangle \tag{40}$$

which was shown to scale linearly with t. The linear behavior was found for all values of p and we obtained $D(p) \propto p$. This result suggests that the individual particles in the lattice gas move as ordinary random walkers; only the tracer diffusion constant is affected by changing p.

It is important to distinguish between *tracer* diffusion and *collective* diffusion. The diffusion constant entering the diffusion equation is the *collective* diffusion constant γ. It is defined as the proportionality constant between an infinitesimal density gradient applied to the system and the response in the particle current.

In our computer simulations, an estimate for γ has been obtained by considering the lattice gas model with periodic boundary conditions in the y direction and introducing a density gradient by applying different p at the two remaining boundaries. This effectively reduces the dimensionality of the system to one dimension. For $p = 10^{-1}$ at the left-hand side and $p = 0$ at the right-hand side, the lattice gas entered a steady state where the density across the system was found to drop linearly. By measuring the average particle current through the system per time step J and the density gradient ∇n, we can determine γ by $\gamma = J/(N \nabla n)$, where N is the linear extent of the

lattice. The diffusion constant γ showed a considerable size dependence. For our largest system $N=128$ we obtained $\gamma=1.9$.

Reducing the boundary drive to $p \leqslant 10^{-2}$ on the left-hand side, we obtained a constant density throughout the bulk, but with a density drop in the vicinity of the rightmost border. This result supports diffusive behavior for moderate boundary drives $p \sim 10^{-1}$, while it predicts that in the limit of small p the diffusive description is not valid. This result will be supported further in the succeeding sections, but for now it suffices to draw the parallel back to Fig. 2, which made it clear that the lattice gas showed qualitatively different behavior when p was reduced from $p=10^{-1}$ to $p=10^{-2}$.

4.2. Power Spectrum

We have obtained the power spectrum by Fourier transformation of the time signal for the total number of particles on the lattice. In order to obtain sufficient statistics, it is necessary to perform an ensemble average containing several independent runs. Thus $S(f)$ is obtained by

$$S(f)=\left\langle \left| \sum_{t=1}^{T} \left(\sum_{\mathbf{r}} z(\mathbf{r}, t) \right) \exp(i2\pi ft) \right|^2 \right\rangle \tag{41}$$

The angular brackets denote averaging over many different time series.

Figure 4 shows the power spectrum for the lattice gas for different lattice sizes where the boundary drive is fixed to $p=10^{-1}$. The power spectrum satisfies an algebraic scaling law $S(f) \propto 1/f^{\beta}$, where the exponent $\beta=1$. For the lattice of size 128×128, the scaling region extends for over three orders of magnitude. The deviation from $\beta=1$ is caused by our finite system size as well as a finite time resolution. At high frequencies, the deviation is due to aliasing.[13] The low-frequency crossover to white noise is caused by the finite system size; as the system size increases, the crossover frequency is reduced. [In Section 3.1 we calculated the power spectrum (28) from the linear diffusion equation. The result showed that the power spectrum should scale as $S(f) \propto 1/f$ for f larger than the frequency f_c, which is in accordance with the computer simulations.]

From (29) we see that f_c should scale inversely with the volume of the lattice. The crossover frequency f_c can be obtained from the numerical simulations in Fig. 4 by locating the characteristic frequency where the power spectrum exhibits a crossover from $1/f$ noise to white noise, as indicated by the small arrows on Fig. 4. Good agreement with the scaling relation is observed.

The diffusion constant γ which enters the diffusive description can be calculated by substituting numerical values for system size N and crossover

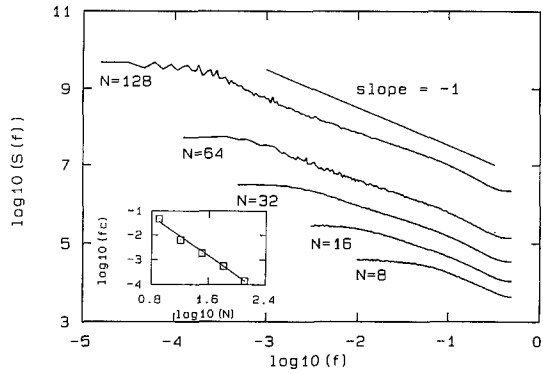

Fig. 4. The power spectrum $S(f)$ for the deterministic lattice gas model for different lattice sizes. It is seen to satisfy algebraic scaling with exponent $\beta = 1$. From the inset it follows that the crossover frequency f_c scales inversely with the volume of the system. The boundary drive is fixed to $p = 10^{-1}$ in all simulations.

frequency f_c into (29). The fact that f_c satisfies the above-mentioned scaling relation implies that γ is independent of system size. Direct evaluation yields $\gamma = 1.4$.

In Section 4.1 the value of the diffusion constant was estimated independently to be $\gamma = 1.9$. However, the use of periodic boundary conditions will, in general, cause an enhanced particle current because we have eliminated the noise from the horizontal borders, which makes it easier for the particles to follow the stream. If the diffusive description is to be taken seriously, we should expect the difference between the two values to disappear in the thermodynamic limit.

The value of the exponent β depends on the strength of the boundary drive. In Fig. 5 the lattice size is fixed to 16×16, while p is varied. As can be seen from the figure, the power spectrum scales as $S(f) \propto 1/f^{\beta}$ at frequencies which are large compared to f_c. However, the exponent exhibits a crossover from $\beta = 1$ for $p > p_c$ to $\beta = 2$ as the boundary drive is reduced from $p = 10^{-1}$ to $p = 10^{-4}$.

This result cannot be explained from the diffusion equation, where we obtained an exponent $\beta = 1$ independent of the free parameters γ and A. Thus, when p is reduced below $p = 10^{-2}$, the diffusion equation does not offer an adequate description of the lattice gas. This conclusion supports the previous observation that the collective diffusion constant was ill defined at small p values.

The dependence of the crossover frequency f_c on p can be obtained from Fig. 5. The crossover frequency is determined as before and we have indicated f_c with small arrows; we get $f_c \propto p$, which is to be expected on

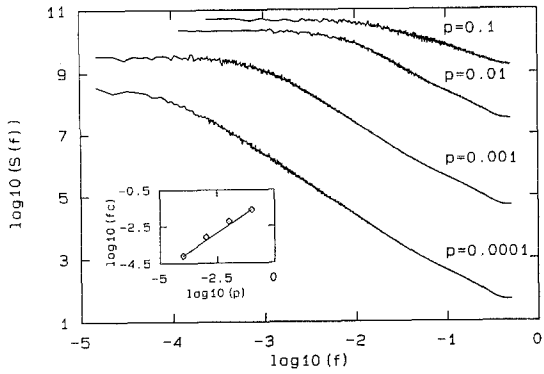

Fig. 5. Power spectrum $S(f)$ for the deterministic lattice gas model. The boundary drive is varied between $p = 10^{-1}$ and $p = 10^{-4}$. Note that the critical exponent exhibits a crossover from $\beta = 1$ to $\beta = 2$ as the boundary drive vanishes. In all simulations we have used a 16×16 lattice.

the following simple-minded argument. We consider a situation where we reduce the boundary drive from p_1 to p_2. Thus the number of particles which are introduced into the lattice is reduced by this ratio p_2/p_1. If we now assume that the qualitative behavior of the lattice gas is unaffected, this reduction can be thought of as redefining our time unit by the reciprocal of this ratio. From this the frequency dependence of p follows. It is interesting that f_c continues to be proportional to p with the same proportionality constant through the region where β changes from 1 to 2.

4.3. Lifetime Distribution

To investigate why the exponents change so dramatically with p, we have calculated the lifetime distribution of the particles. The lifetime distribution is obtained by labeling the particles and following them through each iteration. We record the number of iterations each particle survives in a subsystem of the lattice and calculate the histogram. Thus, if the particle trajectory is given by $\mathbf{r}(t)$, where $\mathbf{r}(t=0) \in \partial\Omega_{\text{sub}}$, we set $t = 0$ when the particle enters over the boundary of the subsystem; the lifetime of the particle is defined as $t' = \max\{t \mid \mathbf{r}(t) \in \Omega_{\text{sub}}\}$. In the numerical simulation, there is no need to average over independent runs, because the system itself is self-averaging, in the sense that new particles are continuously supplied at the boundary, which are incorporated in the statistics.

It is important to use a subsystem, because the activity at the boundary is much higher than in the bulk, due to the white-noise boundary condition. This will overestimate $D(t)$ for small values of t and lead to a

too high value for the α exponent.[6] It should be recognized that the use of subsystems is a computational trick to mask out the initial transient behavior and that the correct α exponent would show up for large system sizes. In all simulations the subsystem chosen is $\Omega_{\text{sub}} = [L/4, 3L/4] \times [L/4, 3L/4]$.

Figure 6 shows the lifetime distribution $D(t)$ for different subsystem sizes when the boundary drive is fixed to $p = 10^{-1}$. We observe that $D(t)$ follows a power law $D(t) \propto 1/t^{\alpha}$ when t is smaller than some crossover time constant t_c, which is indicated by small arrows.

For t larger than t_c we see an exponential decay. The exponent α approaches a constant value $\alpha = 1.5$ independent of the lattice size, and shows some transient behavior for the small systems. [In Section 3.3 we calculated the lifetime distribution (39) from the linear diffusion equation. The result showed that the lifetime distribution should scale as $D(t) \propto 1/t^{3/2}$ for t less than t_c, while $D(t)$ should decay exponentially for t larger than t_c, which is in accordance with the computer simulations.]

In Section 3.3 we defined $t_c = 1/\omega_c$. Thus the crossover time t_c is expected to scale with the volume of the lattice. From the inset of Fig. 6, we see that this is indeed the case.

In the following we examine the consequences of reducing the boundary p on the lifetime distribution.

[6] This effect leads, unfortunately, to an overestimate of the α exponent. See refs. 6 and 24. The power spectrum of the number of particles within the subsystem has the same scaling exponent as for the number of particles on the whole system.

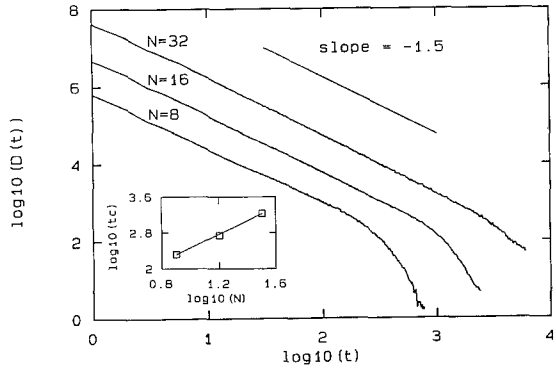

Fig. 6. The lifetime distribution $D(t)$ for different subsystem sizes, with a fixed boundary drive of $p = 10^{-1}$. The lifetime distribution scales as a power law with exponent $\alpha = 1.5$ for $t < t_c$, while for $t > t_c$ we observe an exponential decay. The inset shows the size dependence on the crossover time t_c.

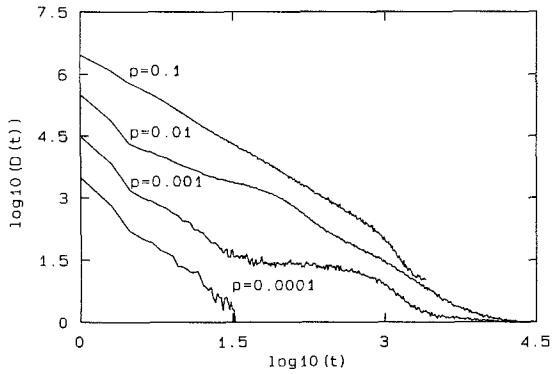

Fig. 7. The lifetime distribution $D(t)$ for a 16×16 subsystem shown for different values of p.

Figure 7 shows the lifetime distribution for a subsystem of size 16×16 for various values of p. For $p = 10^{-1}$ we observe that the lifetime distribution scales according to a power law $D(t) \propto 1/t^{\alpha}$ with exponent $\alpha = 1.5$. This suggests that the particles diffuse through the lattice asymptotically as independent random walkers.

For p in the range $p \in [10^{-2}, 10^{-3}]$ the scaling behavior vanishes and $D(t)$ develops a peak contribution at short lifetimes and a bump at intermediate lifetimes. When p is reduced further to below $p = 10^{-4}$, the lifetime distribution again displays power law behavior, however with an exponent which is slightly higher that before. By increasing the system size, the qualitative behavior for $p \in [10^{-2}, 10^{-3}]$ does not change, while the α exponent for $p = 10^{-4}$ retains its original value $\alpha = 1.5$. The results for $p \in [10^{-2}, 10^{-3}]$ is probably due to finite-size effects and we believe that $\alpha = 1.5$ should hold independently of p.

4.4. Correlation Functions

The equal-time pair correlation function is defined analogously to (30), only the particle density $n(\mathbf{r}, t)$ is substituted by $z(\mathbf{r}, t)$. Hence,

$$C(\mathbf{r}, \mathbf{r}') = \langle [z(\mathbf{r}, t) - \langle z(\mathbf{r}, t) \rangle][z(\mathbf{r}', t) - \langle z(\mathbf{r}', t) \rangle] \rangle \tag{42}$$

The computer simulation poses no complications, except that good statistics is needed. We only consider the case where $\mathbf{r}$ is fixed to the center of the lattice, while $\mathbf{r}'$ is allowed to move horizontally through the lattice. We have simulated the correlation function for the lattice gas for a lattice of size 33×33 for three different boundary drives, $p = 10^{-1}$, $p = 10^{-2}$, and $p = 10^{-3}$. In the case of the correlation function it is important to use an

odd number of lattice sites in the system. This comes from the fact that the boundary conditions on a finite lattice must be such that the four ordered structures of cubic symmetry can exist as a monodomain on the lattice.

The results are shown in Fig. 8. The correlation function is seen to be symmetrical around the center of the lattice, which reflects that our system has inversion symmetry. From our central peak, the function oscillates from even to odd lattice sites with a decreasing amplitude. This behavior is expected on the following grounds. Assume that the site at the center is occupied, $z(L/2, L/2) = 1$. Thus, the particle is part of a particular domain of cubic symmetry. The characteristic size of the domain is called the correlation length ξ. As we let $\mathbf{r}'$ scan horizontally through the lattice, the correlation function will reflect the cubic symmetry of the ordered domain. In a simple theory we would expect the correlation function to exhibit an Ornstein–Zernike type of behavior,[25] where the amplitude of the correlation function is exponentially damped as $\exp(-|\mathbf{r}-\mathbf{r}'|/\xi)$.

The oscillatory behavior is, however, different for the three boundary drives. For $p = 10^{-1}$ the oscillation is damped after approximately $\xi = 2$ lattice sites, while for $p = 10^{-2}$ the correlation function continues to oscillate all the way from the center of the lattice to the border: this corresponds to a long-range order of particles sitting in a regular grid, in accordance with our discussion in Section 2. This feature is even more pronounced for $p = 10^{-3}$, where the amplitude is larger.

The general behavior of the correlation function for different values of the driving field p thus resembles the situation one would expect for a thermodynamic system, where the driving field is substituted by the temperature. The divergence of the correlation length as $p \to 0$ could be

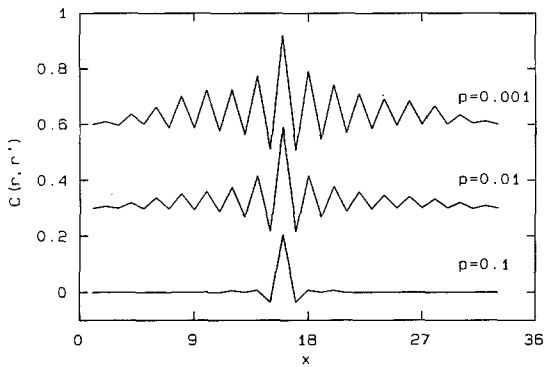

Fig. 8. Spatial correlation function $C(\mathbf{r}, \mathbf{r}')$ for the deterministic lattice gas model. The boundary drive is varied between $p = 10^{-1}$ and $p = 10^{-3}$. In all simulations we have used a 33×33 lattice. The correlation functions for $p = 10^{-2}$ and $p = 10^{-3}$ are displaced vertically by 0.3 and 0.6, respectively.

interpreted as a phase transition. We will return to this point in the next section.

In Section 3.2 we calculated $C(\mathbf{r}, \mathbf{r}')$ from the diffusion equation. Returning to Fig. 3, we see pronounced oscillations, with a wavelength of one lattice constant. The origin of these is, however, completely different, as explained. The similarity between the two correlation functions is, apart from the central peak, merely accidental and we are led to the conclusion that we cannot pursue the diffusive description to account for the fine details in the lattice gas model.

4.5. Structure Factor

We have seen in Section 4.4 that the diffusive description of the lattice gas is invalidated for $p < p_c$, where we have estimated p_c to be in the range $p_c \in [10^{-2}, 10^{-1}]$. If the crossover in the critical β exponent is associated with a kind of phase transition at $p = p_c$, this should be detected in the structure factor.

The structure factor $S(\mathbf{q})$ is defined as the Fourier transform of the density–density correlation function $C(\mathbf{r}, \mathbf{r}')$,

$$S(\mathbf{q}) = \frac{1}{N^2} \sum_{\mathbf{r}} \sum_{\mathbf{r}'} \exp[-i2\pi\mathbf{q} \cdot (\mathbf{r} - \mathbf{r}')]\, C(\mathbf{r}, \mathbf{r}') \tag{43}$$

The structure factor $S(\mathbf{q})$ can in principle be evaluated for all $\mathbf{q}$ vectors, but if the finite system Ω is extended to infinity by means of periodic boundary conditions, it can easily be shown that only the q-vectors $\mathbf{q} = (h/L, k/L)$, where $(h = 0, ..., N)$ and $(k = 0, ..., N)$, give a nonzero contribution to the structure factor.

In the computer simulations it is more convenient to formulate the structure factor in a slightly different way. Following ref. 25, we obtain

$$S(\mathbf{q}) = \frac{1}{N^2} \left\langle \left| \sum_{\mathbf{r}} \exp(-i2\pi\mathbf{q} \cdot \mathbf{r})\, z(\mathbf{r}, t) \right|^2 \right\rangle \tag{44}$$

The formation of domains of cubic symmetry should show up as a peak in $S(\mathbf{q})$ for $\mathbf{q} = (1/2, 0)$. Thus, it is sufficient to calculate $S(\mathbf{q})$ for a scan along the q_x axis. The results are shown on Fig. 9 for a 33×33 system with $p = 10^{-1}$, $p = 10^{-2}$, and $p = 10^{-3}$. This corresponds to the parameters used in Fig. 3. The solid curves through the data points represent a least square fit to a Lorenz function. From the fit we obtain the full-width half-maximum w of the peaks. The correlation length ξ can be estimated from w by $\xi = 1/w$.

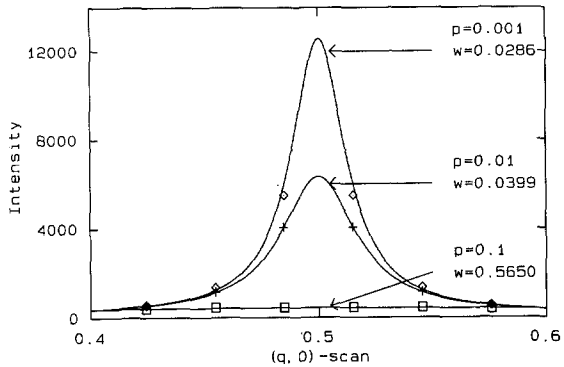

Fig. 9. Structure factor for a 33×33 lattice for different values of p. The structure factor $S(\mathbf{q})$ shows a diffuse peak around $\mathbf{q} = (1/2, 0)$. The width of the peak decreases with p, indicating that as $p \to 0$, larger and larger domains form.

From the results we see that there is a dramatic increase in the correlation length, from $p = 10^{-1}$ ($\xi \sim 2$) to $p = 10^{-2}$ ($\xi \sim 25$). For $p \leqslant 10^{-3}$ the correlation length exceeds the system size.

For a thermodynamic system undergoing a second-order phase transition, the correlation length diverges as $T \to T_c$. Thus, for a finite system we expect the correlation length $\xi(T)$ to obtain its maximum value for $T = T_c$. From Fig. 9, we see that the correlation length continues to increase as p is reduced below p_c, which indicates that the phase transition occurs at $p = 0$ and not at $p = p_c$.

This implies that the crossover is not induced by a phase transition, as we know from the standard theory of critical phenomena, but rather by the dynamics, as will be explained in the next section.

4.6. Crossover

The change in the fluctuation spectrum from a $1/f$ spectrum to a $1/f^2$ spectrum occurs as the density $n = n(p)$ on the system becomes so small that system loses its dynamical connectedness across the lattice. The density as a function of the introduction probability p can easily be estimated. In steady state, the in- and outflux of particles over the edge are equal. The probability for a particle to enter the lattice is, to leading order, $p(1-n)$. First, the particle should enter an edge site, which happens with probability p. In order for the particle to be able to move from the edge site into the lattice, the neighbor site has to be empty; this occurs with probability $1-n$. The probability for a particle to leave the system is, to leading order, equal to $n(1-p)n$. The particle has to sit in a site next to the edge site; this give

us one factor n; furthermore, the particle has to have a nearest neighbor in the direction onto the lattice, which is there with probability n, and finally the nearest neighbor site on the edge should be vacant, which gives another factor $1-p$.

The solution $n(p)$ to the equality $p(1-n)=n^2(1-p)$ is plotted in Fig. 10, together with the measured density. One observes that the density converges to a value of about 1/4 as p becomes smaller than about 10^{-1}. At this density, no particle needs to have any nearest neighbor, and hence the particle system cannot lower its density further by its own repulsive interaction. The particle system is not able to support density waves across the system for these low densities.

In order to quantify this crossover in the dynamical connectedness, we have measured the distribution of damage clusters of the system as a function of p. The damage clusters are defined as follows. The system is first taken into the stationary state. Next two parallel runs are made from initial configurations which only differ by the location of one single particle which has been placed in one of the edge sites. The system is simulated a number of time steps equal to the linear size N of the lattice. This number of time steps will suffice for allowing a perturbation to transverse the system if a dynamical connection exists across the lattice. By comparing the two runs, we are able to identify the number s of lattice sites which have been influenced by the extra particle. These sites define a damage cluster of size s. During these N time steps, no particles are allowed to leave or enter the system over the edge.

By repeating this procedure, we can measure the size distribution $D(s)$ of the damage clusters. Figure 11 shows a semilogarithmic plot of the dis-

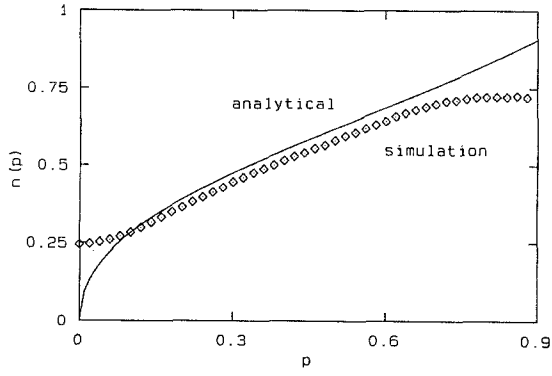

Fig. 10. The density $\langle n(p)\rangle$ as a function of the boundary drive p from computer simulation and analytical calculations.

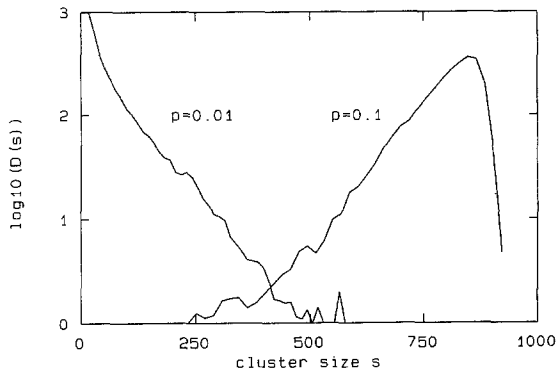

Fig. 11. The size distribution $D(s)$ of damage clusters shown on a semilogarithmic plot for the boundary drive $p = 10^{-1}$ and $p = 10^{-2}$. The system size is 32×32. The main contribution to the distribution is shifted toward lower cluster sizes as p is reduced, signaling a crossover in dynamical connectivity.

tribution for two different values of p. The first distribution is measured with $p = 10^{-2}$, which is in the low-drive region in the sense that the average density is about 1/4 and that the power spectrum exponent β is about to crossover from the value 1 to the value 2. The distribution exhibits approximately an exponential behavior. The other distribution is measured with $p = 10^{-1}$. This distribution is very broad with support at cluster sizes all the way up to the total system size. For this p value, $\beta = 1$ and $n(p)$ is slightly larger than 1/4.

We have studied the size dependence of the average cluster size per time step $\bar{s} = \langle s \rangle / N$. The motivation for considering this quantity is as follows. If the whole system happens to be ordered in the cubic pattern discussed at the end of Section 2, a damage cluster is always of size N. Hence $\bar{s} = 1$. As soon as the system becomes connected, the number of sites in a damage cluster $s(t)$ after t time steps may grow exponentially like $s(t) \sim a^t$ with a equal to the average number of nearest neighbors, i.e., $1 < a < 4$. Our simulations show that in the small-p region, $\bar{s}$ stays finite at a value of order one as the system size is increased. For p larger than 10^{-1}, $\bar{s}$ grows with the system size. The nature of this crossover is the subject of current investigations.

5. THE PERIODIC LATTICE GAS MODEL

The periodic lattice gas model is defined in analogy with the previous lattice gas model, with the exception that the open boundary is substituted by periodic boundary conditions. In this manner we obtain a pure model,

without a surface, and with translational symmetry, both vertically and horizontally. The total number of particles is conserved, and it should be noticed that when $\langle z(\mathbf{r}, t)\rangle \leqslant 0.5$, there is a possibility that the activity stops, because no particle repels any other. However, this is not likely to happen, and was only observed for $\langle z(\mathbf{r}, t)\rangle < z_c$, where $z_c \approx 0.3$. The situation $\langle z(\mathbf{r}, t)\rangle < z_c$ is trivial in the sense that the density is so low that no density fluctuations can be supported, due to the lack of dynamical connectivity in the system.

The power spectrum $S(f)$ is calculated as the Fourier transform of the total number of particles inside a subsystem, while the lifetime distribution is calculated as before. The size of the subsystem is chosen to be $\Omega_{\text{sub}} = [L/4, 3L/4] \times [L/4, 3L/4]$. The results for the power spectrum are shown in Fig. 12, while the corresponding results for the lifetime distribution are shown in Fig. 13. In the simulations we used a fixed particle density $\langle z(\mathbf{r}, t)\rangle = 0.3$, which corresponds to the density for the boundary-driven system at $p = 10^{-1}$, as can be seen from Fig. 10.

It follows that both $S(f)$ and $D(t)$ for the periodic lattice gas model display power law scaling with exponents corresponding to the case $p > p_c$ for the boundary-driven model. Further, the exponents proved to be independent of the particle density $[\langle z(\mathbf{r}, t)\rangle > z_c]$.

The correlation function $C(\mathbf{r}, \mathbf{r}')$ has been calculated for $\langle z(\mathbf{r}, t)\rangle > z_c$. The results are compatible with those for $p > p_c$.

The observation of $1/f$ fluctuations in the particle number of a subvolume in the completely deterministic periodic lattice gas raises some questions about the applicability of our analytic description. If we assume that the observed power spectrum also in this case is a consequence of boundary-driven diffusion, we need to conclude that the surrounding

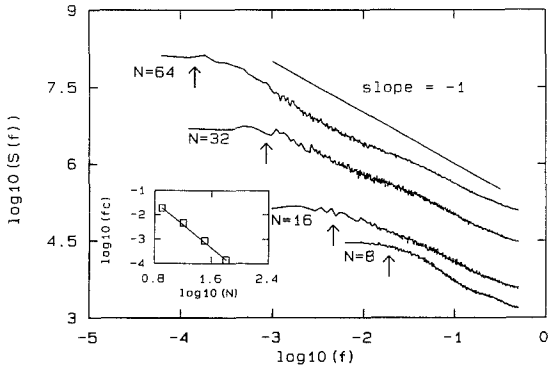

Fig. 12. Power spectrum $S(f)$ for the periodic lattice gas model for different subsystem sizes. The density of particles is fixed to $\langle z(\mathbf{r})\rangle = 0.3$.

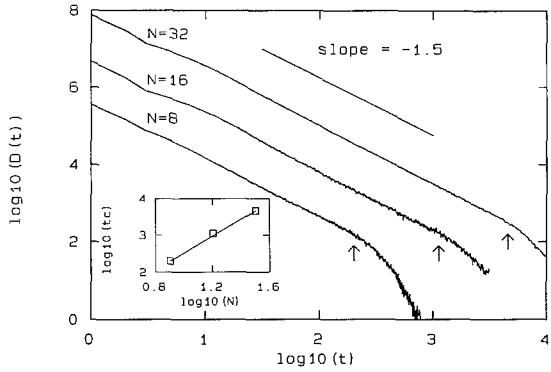

Fig. 13. The lifetime distribution $D(t)$ for the periodic lattice gas model for different subsystem sizes.

system effectively produces a white noise drive of the $z(\mathbf{r}, t)$ at the boundary of the subsystem. [This is certainly consistent with the numerically observed spectrum of the boundary values of $z(\mathbf{r}, t)$, but the power spectrum of the local quantity $z(\mathbf{r}, t)$ for some fixed $\mathbf{r}$ always numerically appears to be white.] However, since the boundary is arbitrarily chosen, a white noise boundary condition for the subsystem seems to be equivalent to a white noise bulk term in the diffusion equation. This lead to an inconsistency, since we know that a white noise bulk term produces a $1/f^{3/2}$ spectrum. We have not yet been able to argue in a convincing way for the form of noise terms to be included in the Langevin equation describing periodic lattice gas.

We should also like to mention that we expect that the fluctuation spectrum of a gas of interacting particles which are allowed to move continuously in space will exhibit $1/f^{3/2}$ as soon as the particle trajectories become chaotic. The restriction to a discrete lattice hinders the lattice gas particles from developing truly chaotic trajectories, although, as indicated by the lifetime distribution, the particles do behave at long times as random walkers. This point is currently under investigation by the use of molecular dynamics simulations of particles moving in the continuous plane.

6. CONCLUSION

We have presented a detailed analysis of $1/f$ fluctuations in a lattice gas in which particles move according to deterministic rules. Two realizations of the model have been studied: a completely deterministic periodic model and an open system with a stochastic drive at the boundary. In both

models we observe a $1/f$ power spectrum for the density fluctuations within a subvolume.

The simulation results were compared to analytic results derived from a macroscopic Langevin description in terms of a simple diffusion equation subject to a white noise boundary condition. It is important to emphasis that this description does not include any fluctuating bulk source term.

The $1/f$ spectrum found in the case of deterministic dynamics is in contrast to results for lattice gases driven by Monte Carlo dynamics. The density fluctuation spectrum for such models has previously been found to exhibit a power spectrum which scales as $1/f^{3/2}$.[7] Such fluctuations can be described by the use of a diffusion equation in which a conserving bulk noise term is included.[14, 20]

Although the deterministic and the stochastic lattice gases have different density fluctuations, the individual particles do, in both cases asymptotically, perform ordinary random walks. The difference between the two models consist in different correlations among the particles. In the deterministic model, the particles remain correlated, whereas in the stochastic case, correlations are lost with time. This shows up in the following way. Strictly independent particles will fulfill the scaling relation $\alpha + \beta = 3$, where the lifetime scales as $D(t) \sim 1/t^{\alpha}$ and the power spectrum scales as $S(f) \sim 1/f^{\beta}$.[9] This scaling relation is found to be fulfilled for the stochastic lattice gas, whereas the deterministic gas has $\alpha = 3/2$ and $\beta = 1$.

It is interesting to investigate in more detail the connection between the microscopic dynamics and the form of the fluctuating source term to be included in an effective Langevin diffusive description. We have found that deterministic dynamics on a lattice is to be described without a fluctuating bulk source term. Does this result change as the trajectories of the particles are allowed to be more complex? We would expect that interacting particles moving in a continuum will produce density fluctuations which need a bulk noise term in the effective Langevin equation as soon as the particle trajectories become chaotic. This issue is currently under investigation.

ACKNOWLEDGMENTS

H. J. J. is supported by the Danish Natural Science Research Council. T. F. is supported by the Danish Research Academy.

REFERENCES

1. J. L. Lebowitz, *Physica* **140A**:232 (1986), and references therein.
2. D. Forster, *Hydrodynamic Fluctuations, Broken Symmetry, and Correlation Functions* (Benjamin, New York, 1975).

3. T. Hwa and Kadar, *Phys. Rev. Lett.* **62**:1813 (1989).
4. G. Grinstein, D.-H. Lee, and S. Sachdev, *Phys. Rev. Lett.* **64**:1927 (1990).
5. Y.-C. Zhang, *Physica A* **170**:1 (1990).
6. H. J. Jensen, *Phys. Rev. Lett.* **64**:3103 (1990).
7. J. V. Andersen, H. J. Jensen, and O. G. Mouritsen, *Phys. Rev. B* **44**:439 (1991).
8. P. Bak, C. Thang, and K. Wiesenfeld, *Phys. Rev. Lett.* **59**:381 (1987).
9. H. J. Jensen, K. Christensen, and H. C. Fogedby, *Phys. Rev. B* **40**:7425 (1989).
10. S. H. Liu, *Phys. Rev. B* **16**:4218 (1977).
11. P. Duta and P. M. Horn, *Rev. Mod. Phys.* **53**:497 (1981).
12. H. J. Jensen, *Physica Scripta* **43**:593 (1991).
13. R. N. Bracewell, *The Fourier Transform and Its Applications* (McGraw-Hill, New York, 1986).
14. G. Grinstein, T. Hwa, and H. J. Jensen, *Phys. Rev. A* **45**:R559 (1992).
15. L. Jacobs and C. Rebbi, *J. Comp. Phys.* **41**:203 (1981).
16. P. M. Morse and H. Feshbach, *Methods of Theoretical Physics* (McGraw-Hill, New York, 1953).
17. G. D. Mahan, *Many-Particle Physics* (Plenum Press, New York, 1990).
18. P. Duchateau and D. W. Zachmann, *Partial Differential Equations* (McGraw-Hill, New York, 1986).
19. S. O. Rice, in *Selected Papers on Noise and Stochastic Processes*, N. Wax, ed. (Dover, New York, 1954).
20. H. C. Fogedby *et al.*, *Mod. Phys. Lett. B* **5**:1837 (1991).
21. D. K. C. MacDonald, *Noise and Fluctuations: An Introduction* (Wiley, New York, 1962).
22. M. Abramowitz and I. A. Stegun, *Handbook of Mathematical Functions* (Dover, New York, 1972).
23. I. S. Gradshteyn and I. M. Ryzhik, *Table of Integrals, Series, and Products* (Academic Press, New York, 1980).
24. H. J. Jensen, *Mod. Phys. Lett.* **5**:625 (1991).
25. H. E. Stanley, *Introduction to Phase Transitions and Critical Phenomena* (Oxford University Press, Oxford, 1971).